The study of the N-Δ Transition GPDs via Exclusive $\pi^{-}\ \Delta^{++}$ Electroproduction

Kyungseon Joo

University of Connecticut

For the CLAS Collaboration

UCONN | UNIVERSITY OF CONNECTICUT

October 19, 2023

clas

Motivations

1. Generalized Parton Distributions (GPDs) are a well-established tool for exploring the 3D structure of the nucleon

2. While extensive studies have been performed for the ground-state nucleon, little is known about the 3D structure of resonances.

3. The nucleon-to-resonance (N->N*) transition GPDs may provide a unique tool for exploring the 3D structure and mechanical properties of nucleon resonances.

Generalized Parton Distributions (GPDs)

$$\rho(x, \vec{k}_T, \vec{b}_T)$$

$$\int d^2 k_T$$

Integrate over transverse ***momentum*** space

Generalized Parton Distributions (GPDs)

3-D nucleon images in the transverse coordinate and longitudinal momentum space

S. Liuti et al., Phys. Rev. D 84, 034007 (2011) (GGL)

P. Kroll et al., Eur. Phys. J. A 47, 112 (2011) (GK)

quark pol.

nucleon pol.

N/q	U	L	T
U	H		$\bar{E}_T$
L		$\widetilde{H}$	$\widetilde{E}_T$
T	E	$\widetilde{E}$	$H_T, \widetilde{H}_T$

$$\bar{E}_T = 2\widetilde{H}_T + E_T$$

Study GPDs: Deeply Exclusive Processes

Deeply Virtual Compton Scattering (DVCS)

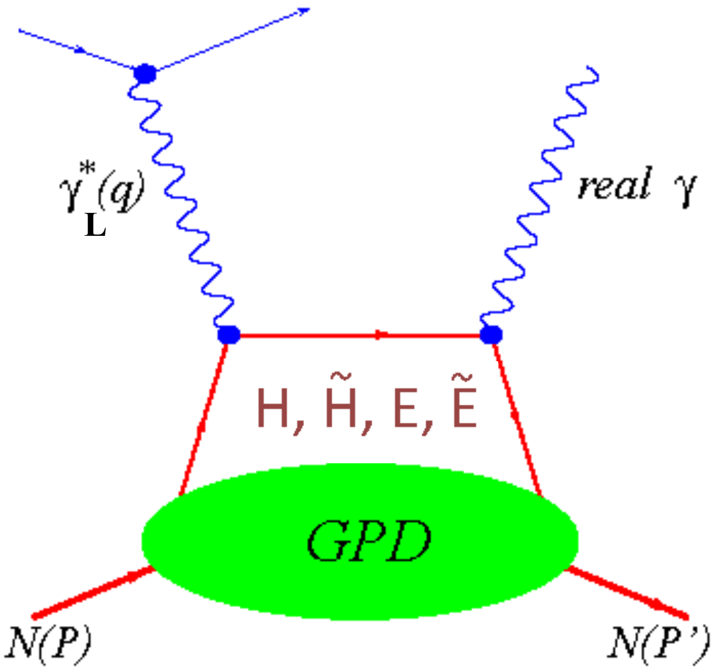

+ Clean process

- 4 twist2 chiral even GPDs: 2 unpolarized and 2 polarized.

Deeply Virtual Meson Production (DVMP)

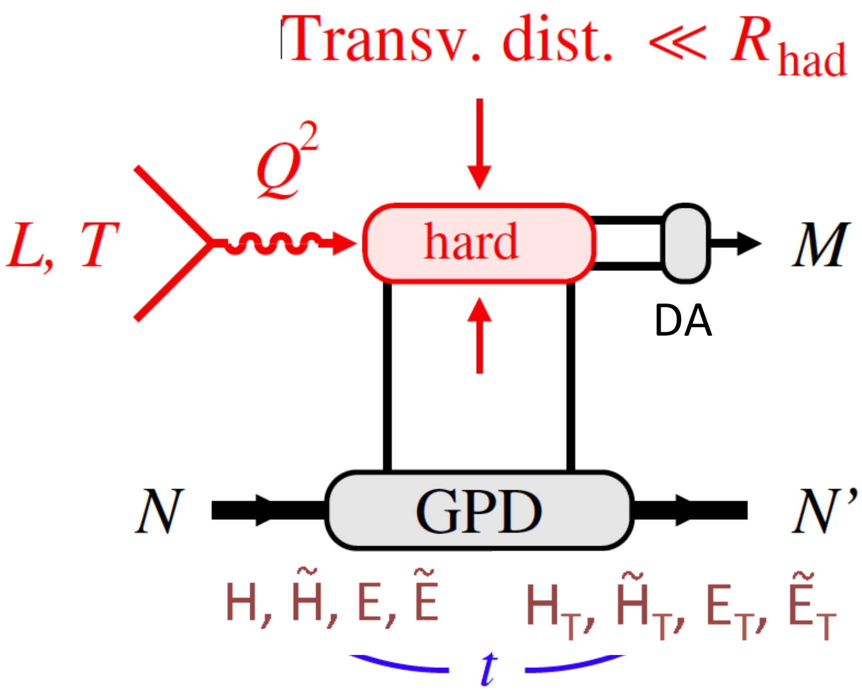

+ Access to transversity degrees of freedom described by chiral-odd GPDs
- Distribution Amplitude (DA) is involved as additional soft non pert. quantity

From the ground state nucleon to resonances

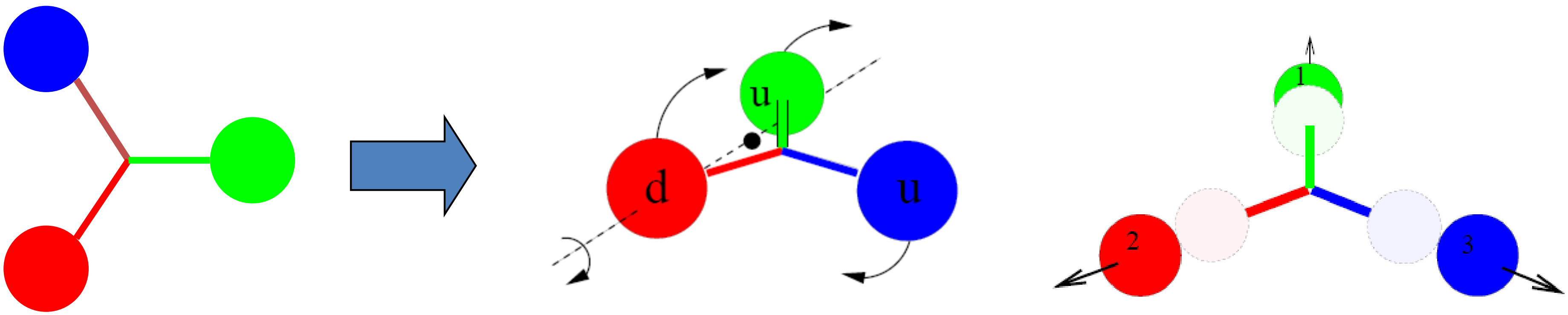

How does the exitation affect the 3D structure of the Nucleon?

→ Pressure distributions, tensor charge, … of resonances?

Traditional way: Study of transition form factors (**2D picture** of transv. position)

3D picture of the exitation process: Encoded in **transition GPDs**

<u>**Simplest case**: N→Δ transition</u> → **16 transition GPDs**

P. Kroll and K. Passek-Kumericki, Phys. Rev. D 107, 054009 (2023).
K. Semenov, M. Vanderhaeghen, arXiv:2303.00119 (2023).

- **8 helicity non-flip transition GPDs (twist 2)**
  - Related to the Jones-Scardon and Adler EM FF for the N → Δ transition
- **8 helicity flip transition GPDs (transversity)**

Non-diagonal DVCS / DVMP

<u>non-diagonal DVCS</u>

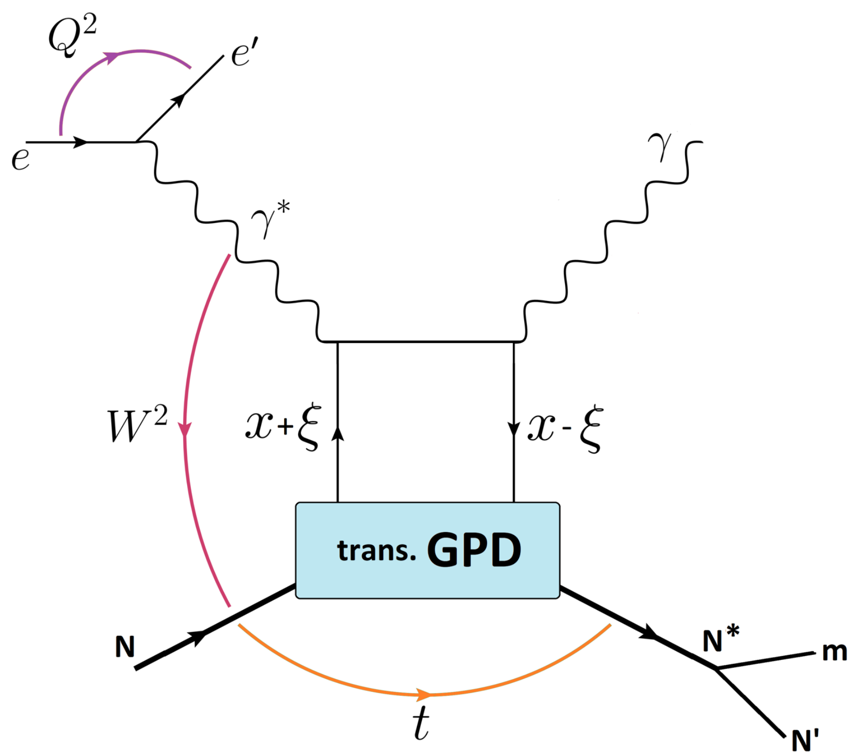

<u>non-diagonal DVMP</u>

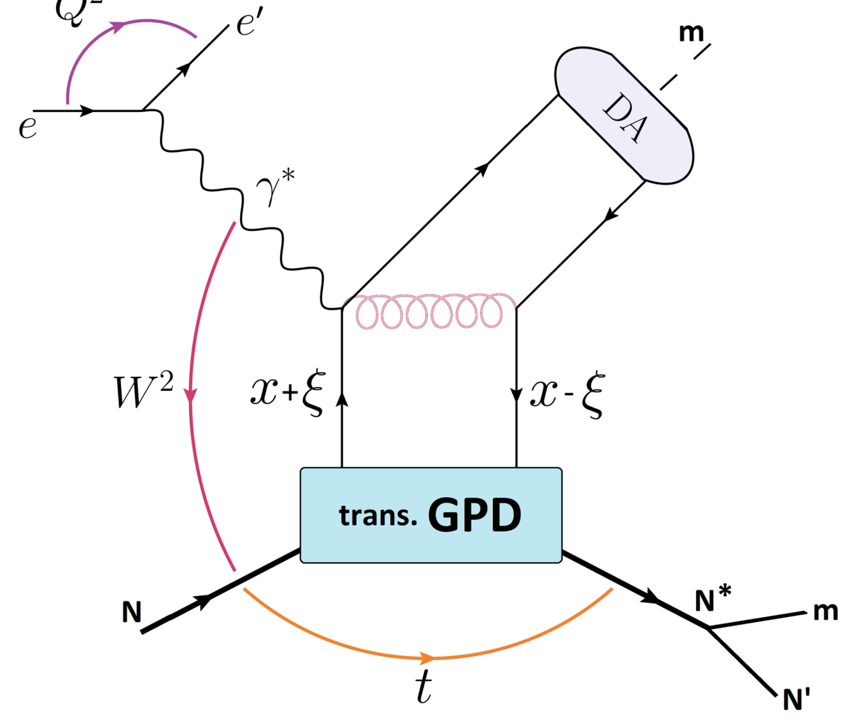

factorization expected for: $-t/Q^2$ small, $Q^2 > M^2_{N*}$ x_B fixed

N->$\Delta(1232)$ transition GPDs: 8 twist-2 GPDs: 4 unpolarized, 4 polarized. K. Semenov, M. Vanderhaeghen, arXiv:2303.00119 (2023)

$$ep \rightarrow e\Delta^{++}\pi^- \rightarrow ep\pi^+\pi^-$$

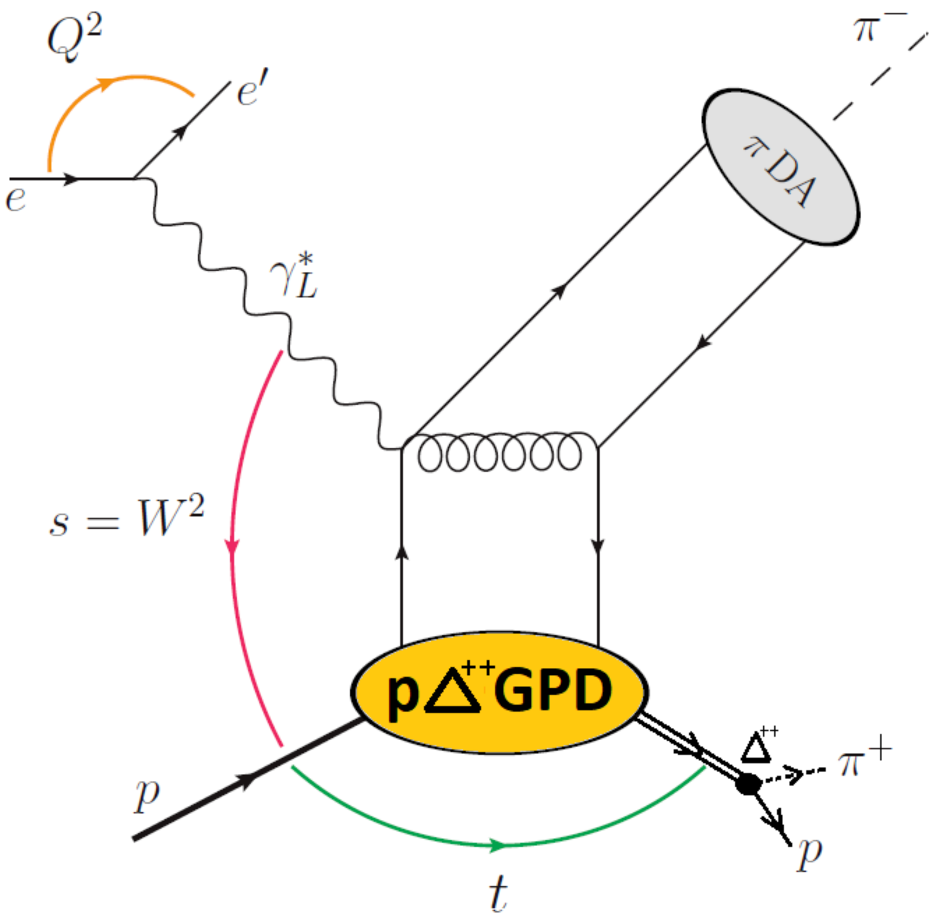

Factorization expected for:

$-t / Q^2 << 1$, x_B fixed, and $Q^2 > M_\Delta^2$

➔ Provides access to p-Δ transition GPDs

➔ 3D structure of the Δ resonance and of the excitation process

PHYSICAL REVIEW LETTERS **131,** 021901 (2023)

First Measurement of Hard Exclusive $\pi^-\Delta^{++}$ Electroproduction Beam-Spin Asymmetries off the Proton

S. Diehl,[34,6] N. Trotta,[6] K. Joo,[6] P. Achenbach,[39] Z. Akbar,[46,12] W. R. Armstrong,[1] H. Atac,[38] H. Avakian,[39] L. Baashen,[11] N. A. Baltzell,[39] L. Barion,[15] M. Bashkanov,[45] M. Battaglieri,[17] I. Bedlinskiy,[28] F. Benmokhtar,[8] A. Bianconi,[42,20] A. S. Biselli,[9] F. Bossù,[4] K.-T. Brinkmann,[34] W. J. Briscoe,[13] D. Bulumulla,[33] V. Burkert,[39] R. Capobianco,[6] D. S. Carman,[39] J. C. Carvajal,[11] A. Celentano,[17] G. Charles,[21,33] P. Chatagnon,[39,21] V. Chesnokov,[36] G. Ciullo,[15,10] P. L. Cole,[25] M. Contalbrigo,[15] G. Costantini,[42,20] V. Crede,[12] A. D'Angelo,[18,35] N. Dashyan,[48] R. De Vita,[17] A. Deur,[39] C. Djalali,[32,37] R. Dupre,[21] M. Ehrhart,[21,*] A. El Alaoui,[40] L. El Fassi,[27] L. Elouadrhiri,[39] S. Fegan,[45] A. Filippi,[19] G. Gavalian,[39] D. I. Glazier,[44] A. A. Golubenko,[36] G. Gosta,[42,20] R. W. Gothe,[37] Y. Gotra,[39] K. Griffioen,[47] K. Hafidi,[1] H. Hakobyan,[40] M. Hattawy,[33,1] T. B. Hayward,[6] D. Heddle,[5,39] A. Hobart,[21] M. Holtrop,[29] I. Illari,[13] D. G. Ireland,[44] E. L. Isupov,[36] H. S. Jo,[24] R. Johnston,[26] D. Keller,[46] M. Khachatryan,[33] A. Khanal,[11] A. Kim,[6] W. Kim,[24] V. Klimenko,[6] A. Kripko,[34] V. Kubarovsky,[39] S. E. Kuhn,[33] V. Lagerquist,[33] L. Lanza,[18,35] M. Leali,[42,20] S. Lee,[1] P. Lenisa,[15,10] X. Li,[26] I. J. D. MacGregor,[44] D. Marchand,[21] V. Mascagna,[42,41,20] G. Matousek,[7] B. McKinnon,[44] C. McLauchlin,[37] Z. E. Meziani,[1,38] S. Migliorati,[42,20] R. G. Milner,[26] T. Mineeva,[40] M. Mirazita,[16] V. Mokeev,[39] P. Moran,[26] C. Munoz Camacho,[21] P. Naidoo,[44] K. Neupane,[37] S. Niccolai,[21] G. Niculescu,[23] M. Osipenko,[17] P. Pandey,[33] M. Paolone,[30,38] L. L. Pappalardo,[15,10] R. Paremuzyan,[39,29] S. J. Paul,[43] W. Phelps,[5,13] N. Pilleux,[21] M. Pokhrel,[33] J. Poudel,[33,†] J. W. Price,[2] Y. Prok,[33] A. Radic,[40] B. A. Raue,[11] T. Reed,[11] J. Richards,[6] M. Ripani,[17] J. Ritman,[14,22] P. Rossi,[39,16] F. Sabatié,[4] C. Salgado,[31] S. Schadmand,[14] A. Schmidt,[13,26] Y. G. Sharabian,[39] U. Shrestha,[6,32] D. Sokhan,[4,44] N. Sparveris,[38] M. Spreafico,[17] S. Stepanyan,[39] I. Strakovsky,[13] S. Strauch,[37] M. Turisini,[16] R. Tyson,[44] M. Ungaro,[39] S. Vallarino,[15] L. Venturelli,[42,20] H. Voskanyan,[48] E. Voutier,[21] D. P. Watts,[45] X. Wei,[39] R. Williams,[45] R. Wishart,[44] M. H. Wood,[3] M. Yurov,[27] N. Zachariou,[45] Z. W. Zhao,[7,33] and M. Zurek[1]

(CLAS Collaboration)

CLAS12 at JLAB

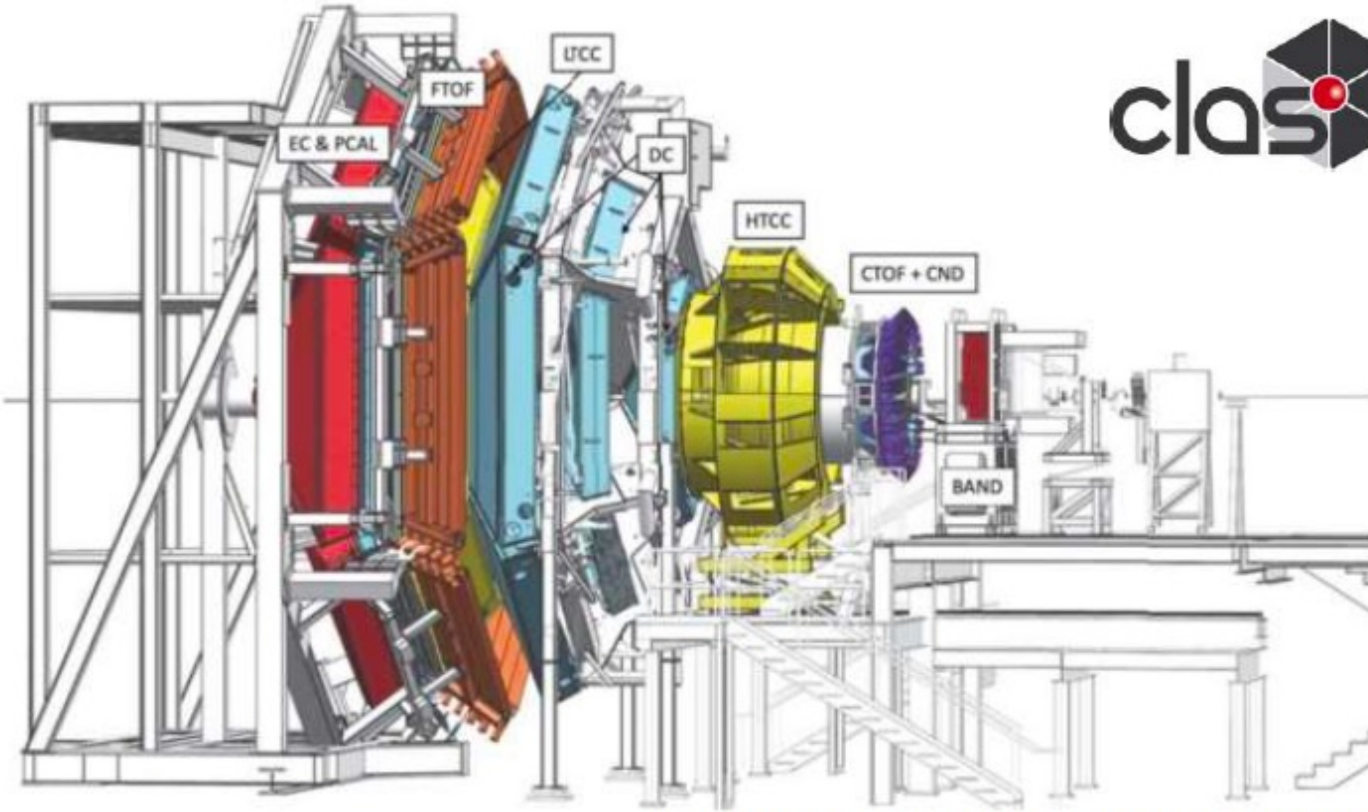

V. Burkert et al., Nucl. Instr. Meth. A 959, 163419 (2020)

- ➔ Data recorded with CLAS12 during fall 2018 and spring 2019 (RG-A)
  - ➔ 10.6 GeV / 10.2 GeV electron beam ~ 86 % average polarization
  - ➔ liquid H_2 target

Event Selection and Kinematic Cuts

Event selection: $ep \rightarrow ep\pi^- X$

$$X = \pi^+$$

➔ 2 sigma cut around the missing π^+

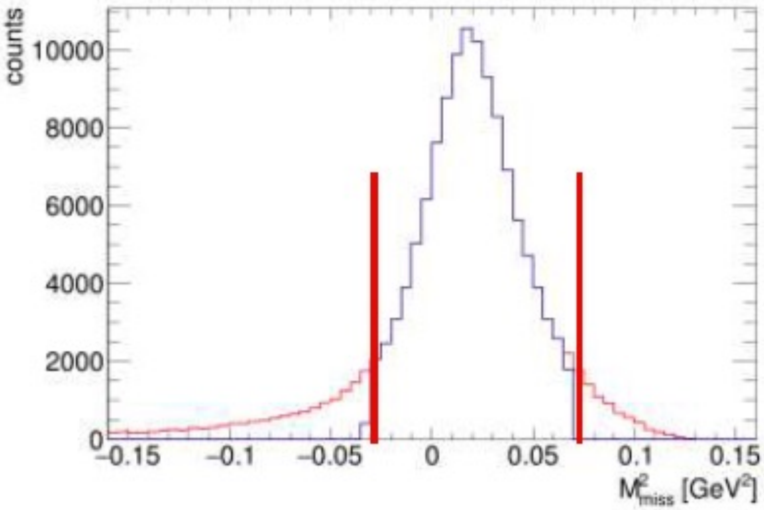

Kinematic cuts:

$Q^2 > 1.5$ GeV^2 $W > 2$ GeV

$y < 0.75$ $-t < 1.5$ GeV^2

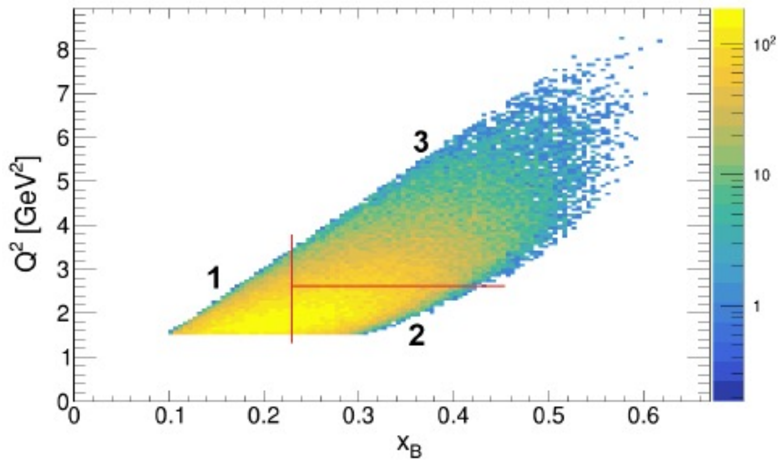

Event Selection and Background Rejection

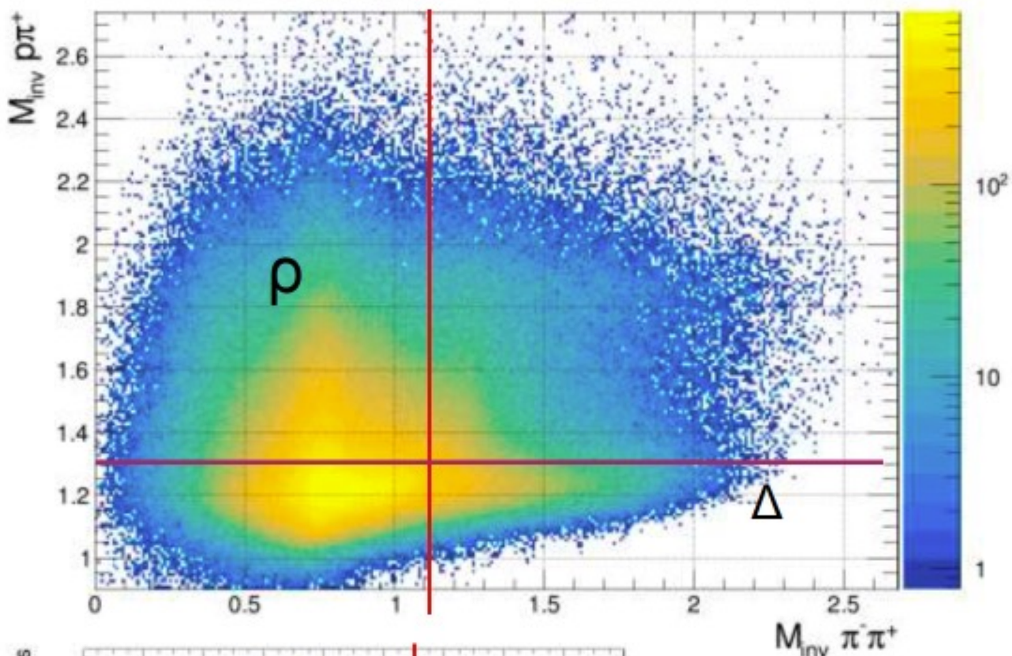

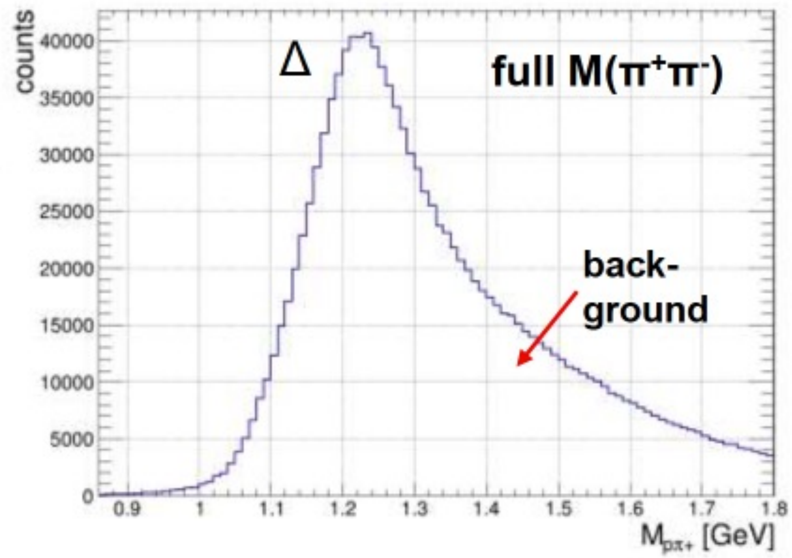

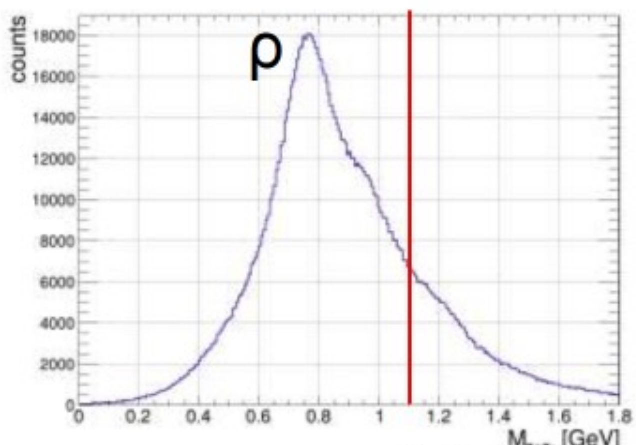

$ep \rightarrow ep\rho \rightarrow ep\pi^+\pi^-$

$M(\pi^+\pi^-) > 1.1$ GeV

ρ contamination

< 0.8 %

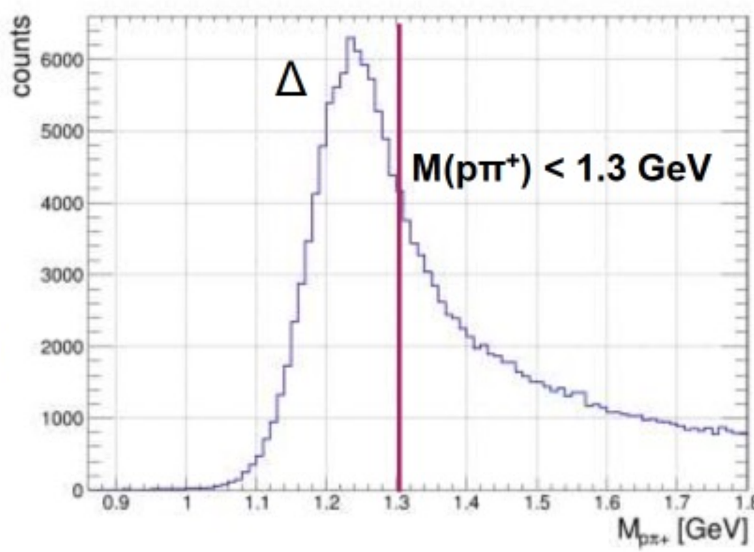

Monte Carlo Simulations

2 MC samples have been used:

a) Background: Semi-inclusive DIS MC

- Does not contain the $\pi^-\Delta^{++}$ production in „forward“ kinematics
- Contains nonres. background as well as ρ production and other potential background channels
- Used to estimate background shape and contaminations

b) Signal: Exclusive $\pi^-\Delta^{++}$ MC

- Phase space simulation with a weigth added to match experimental data
- Δ peak with PDG mass and FWHM

➔ Both MCs are processed through the full simulation and reconstruction chain

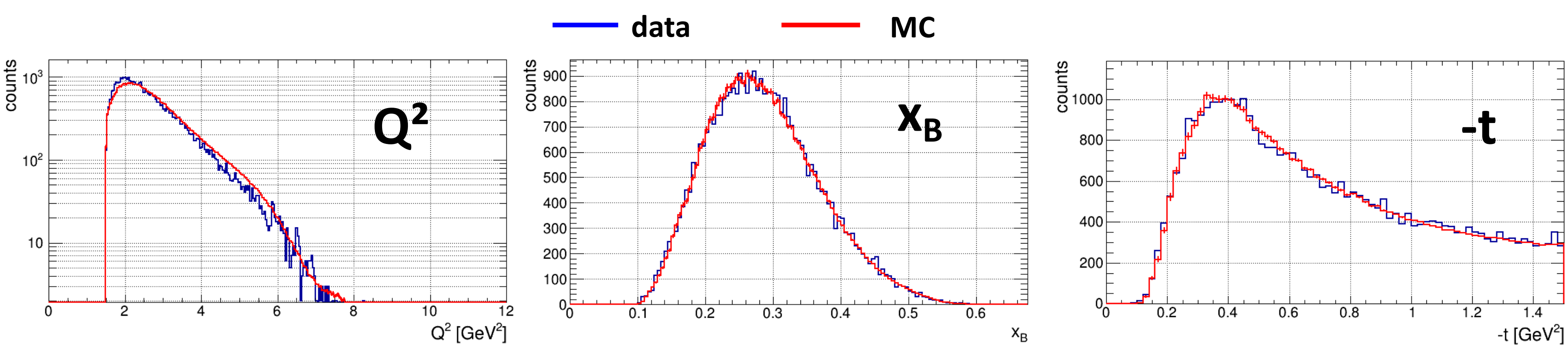

Signal and Background Separation

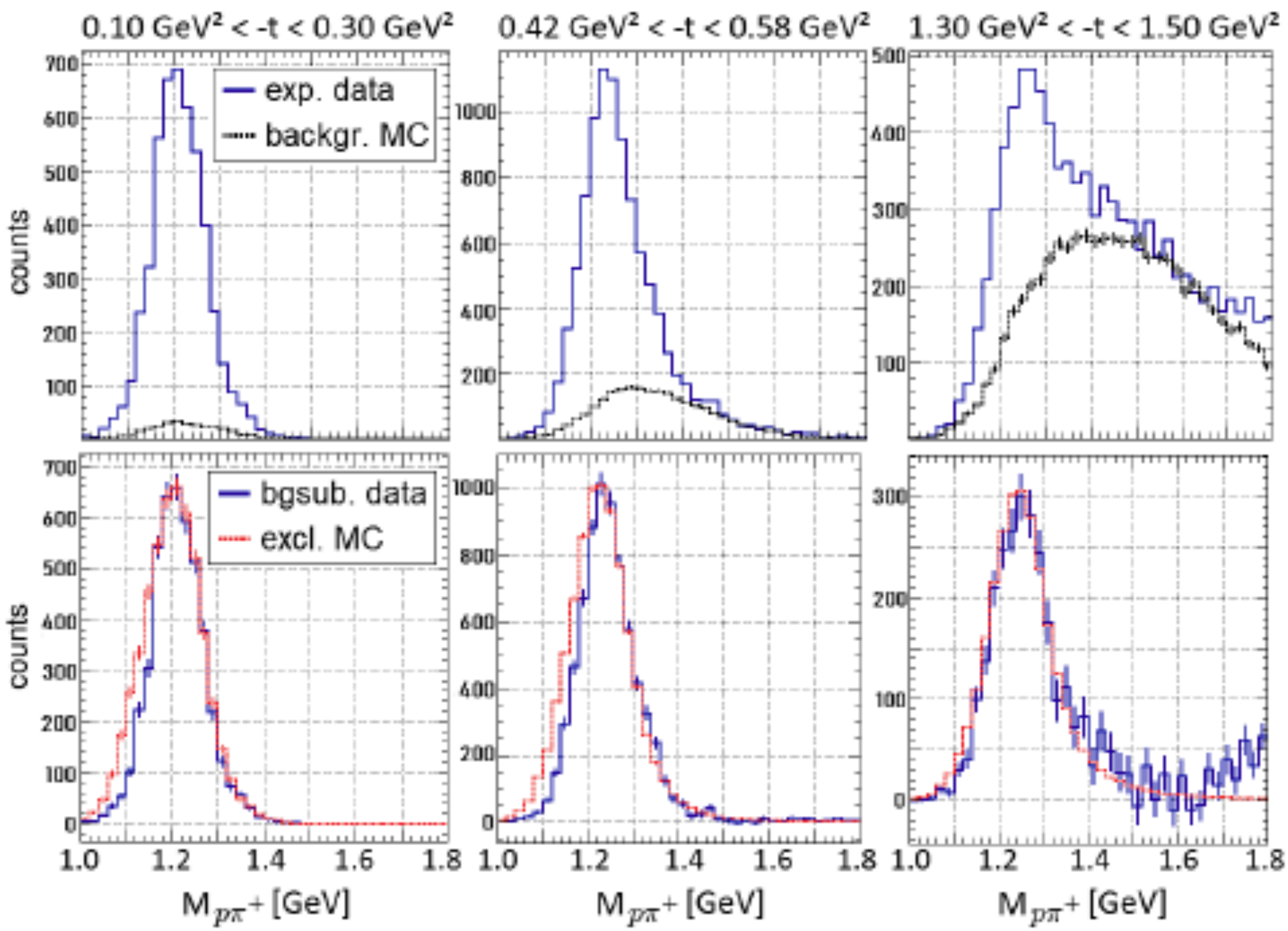

Resulting Beam Spin Asymmetries (Q^2-x_B integrated)

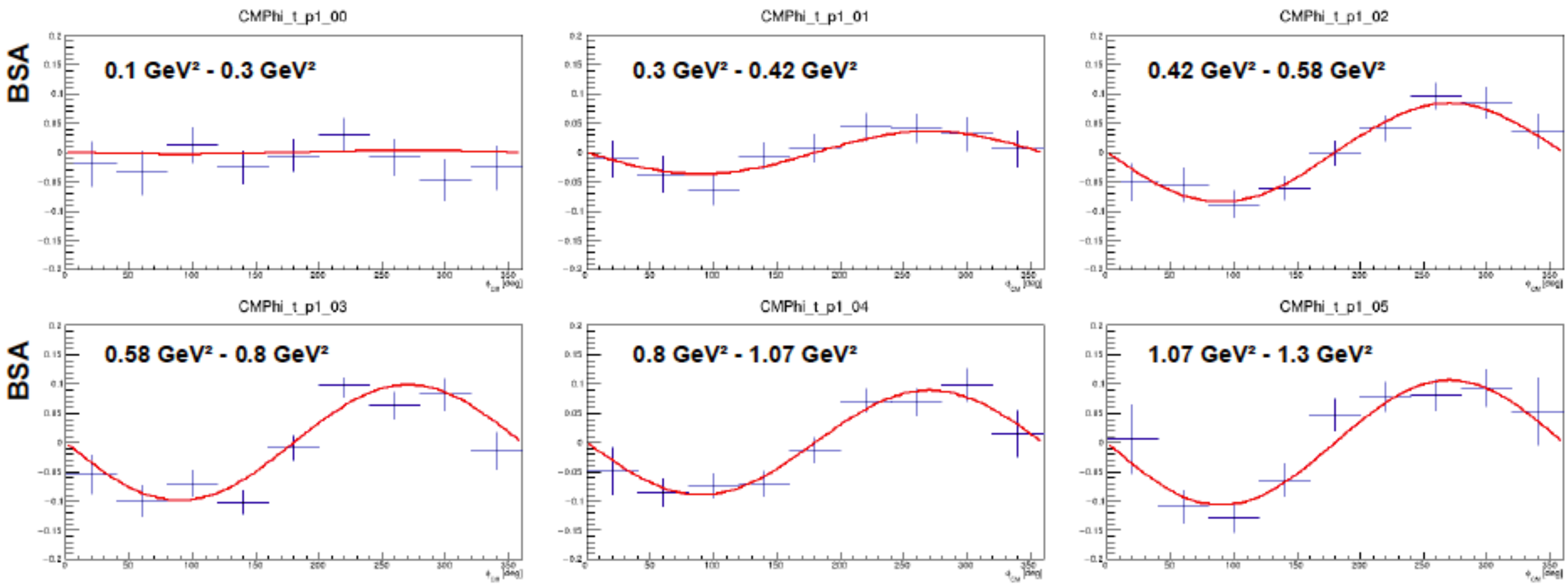

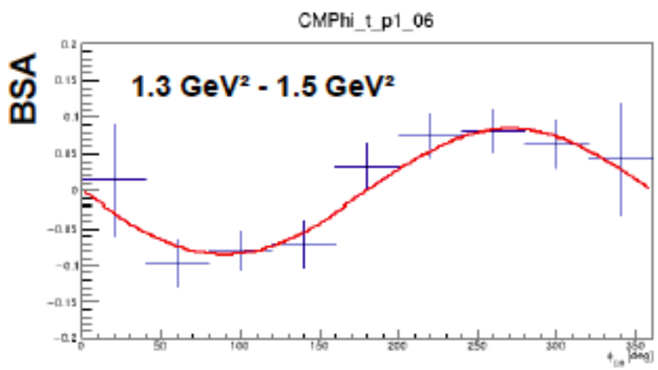

$$BSA_i = \frac{1}{P_e}\frac{N_i^+ - N_i^-}{N_i^+ + N_i^-} \sim \sqrt{2\epsilon(1-\epsilon)}\frac{\sigma_{LT'}}{\sigma_0}\sin\phi$$

Results

S. Diehl et al. (CLAS collab.),
Phys. Rev. Lett. 131, 021901 (2023)

S. Diehl et al. (CLAS collab.)
Phys. Lett. B 839, 137761 (2023)
A. Kim, submitted to PLB

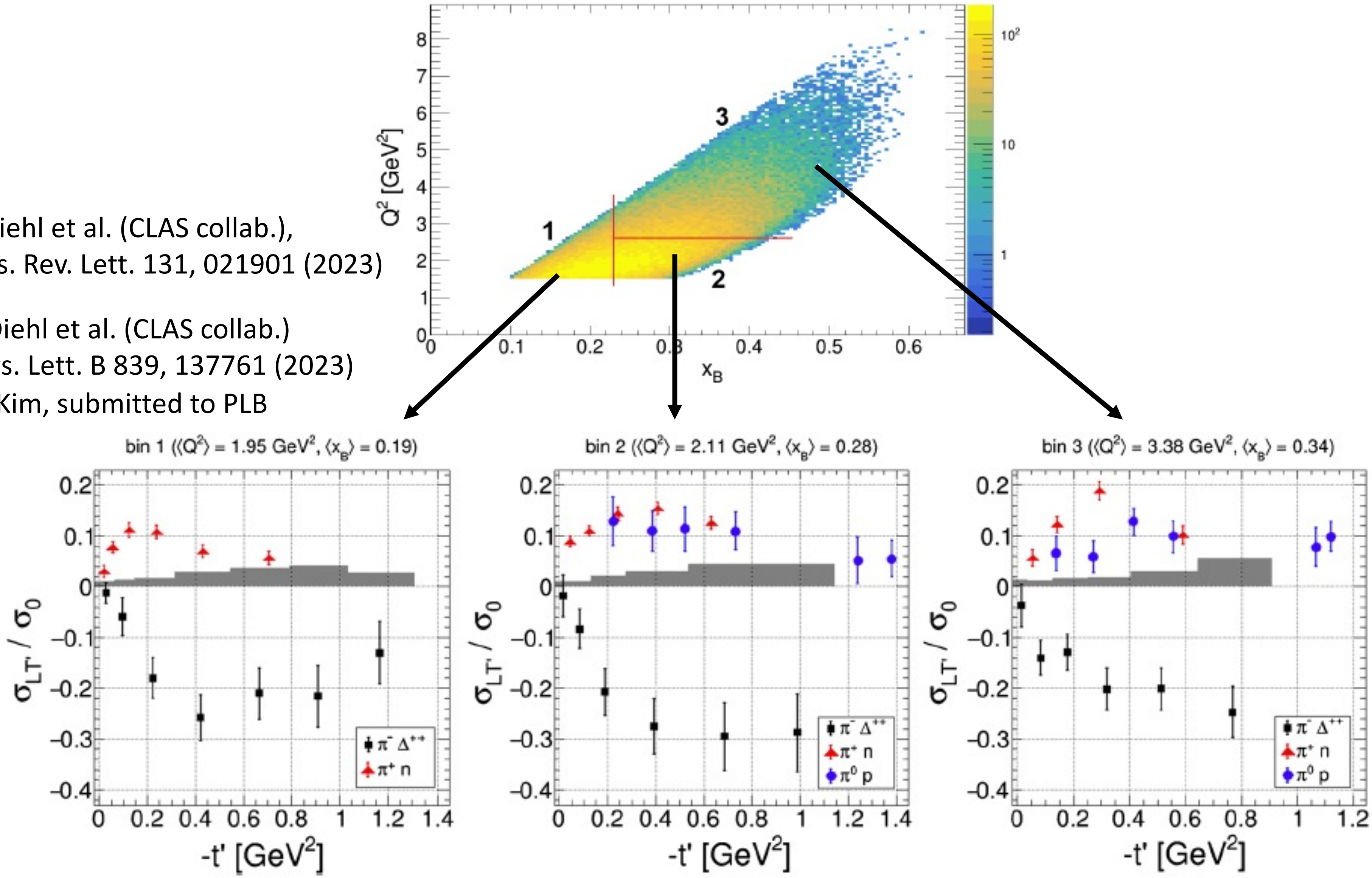

Outlook and Next Steps

non-diagonal DVCS

$$e\,p \rightarrow e'\,\Delta^{+}\,\gamma \rightarrow e'\,n\,\pi^{+}\,\gamma$$

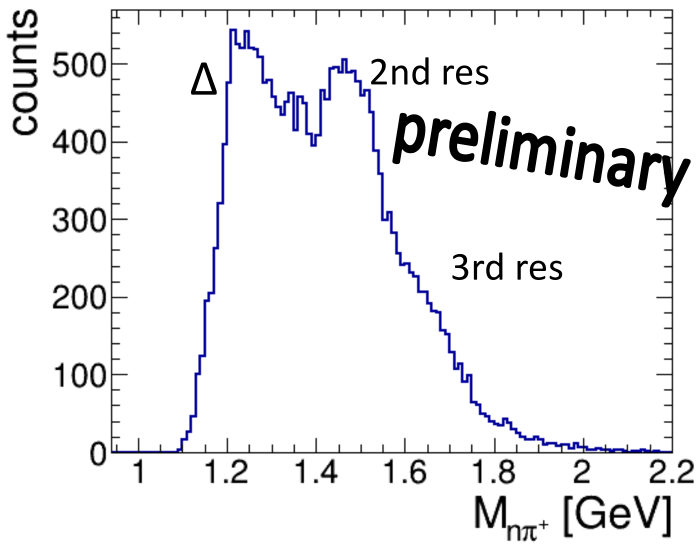

Other non-diagonal DVMP channels

$$ep \rightarrow e\Delta^{0}\pi^{+} \rightarrow e(p\pi^{-})\pi^{+}$$

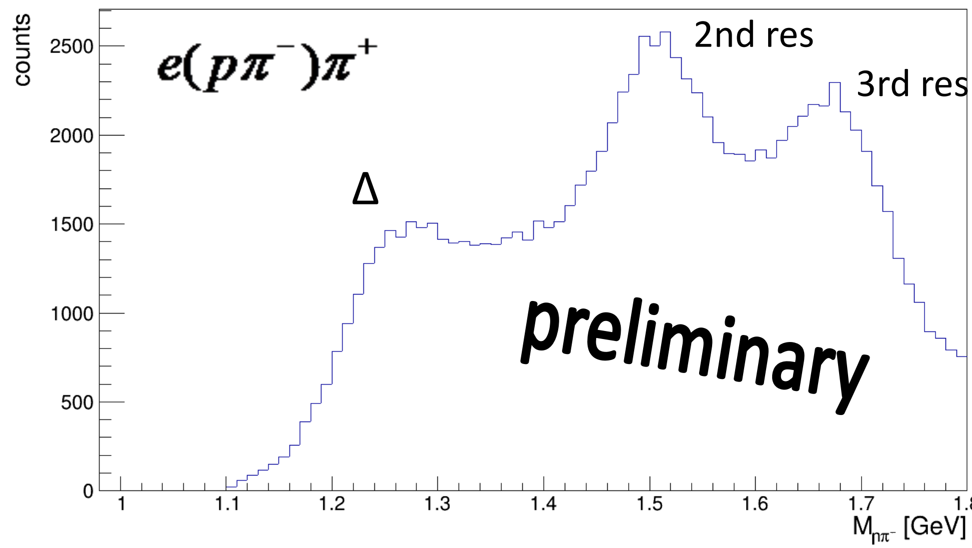

$$ep \rightarrow e\Delta^{++}\pi^{-} \rightarrow e\underbrace{p\pi^{+}}_{I_z = +3/2}\pi^{-}$$

➔ The $p\pi^{+}$ final state can **only** be populated by **Δ-resonances**

- Large gap between Δ(1232) and higher resonances

Non-Diagonal DVCS

$$e\,p \rightarrow e'\,\Delta^+\,\gamma \rightarrow e'\,n\,\pi^+\,\gamma$$

Kinematic cuts: $W > 2$ GeV $Q^2 > 1$ GeV² $y < 0.8$ $-t < 2$ GeV² $E_{DVCS} > 2$ GeV

Background:

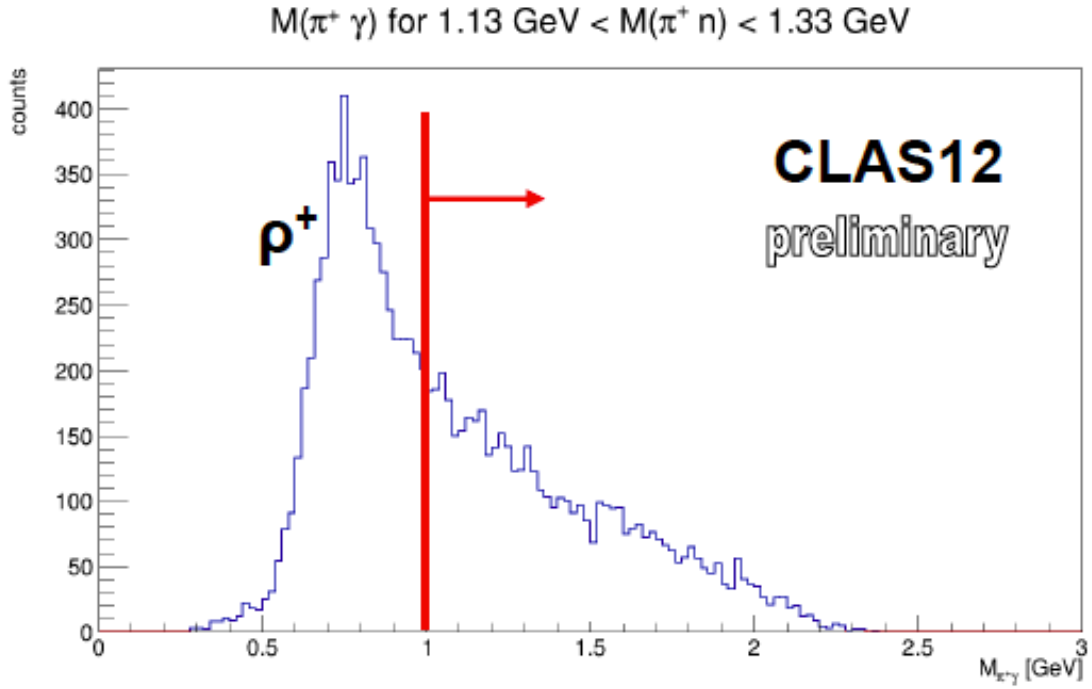

- Dominant background from $\rho^+ \rightarrow \pi^+\,\gamma$

$e\, p \to e'\, \Delta^+\, \gamma \to e'\, n\, \pi^+\, \gamma$

$e\, p \to e'\, \Delta^+\, \gamma \to e'\, n\, \pi^+\, \gamma$

raw — $M(\pi^+\gamma) > 1.0$ GeV

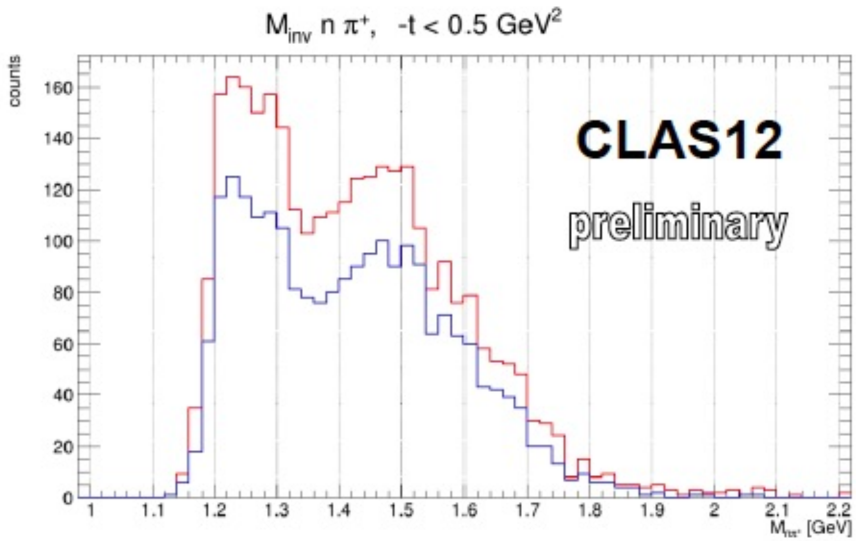

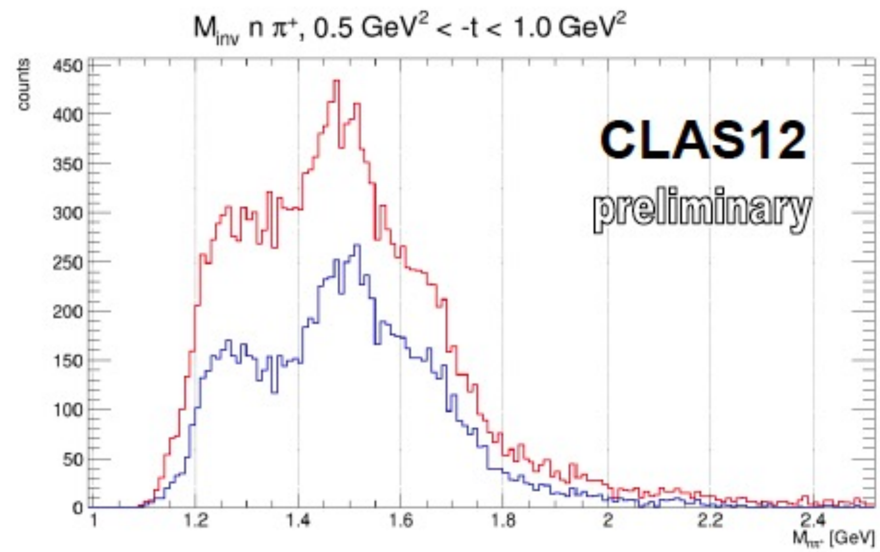

Semenov-Tian-Shansky, Vanderhaeghen, arXiv:2303.00119 (2023)

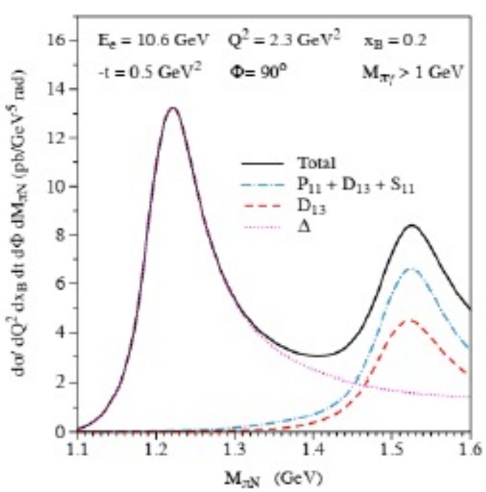

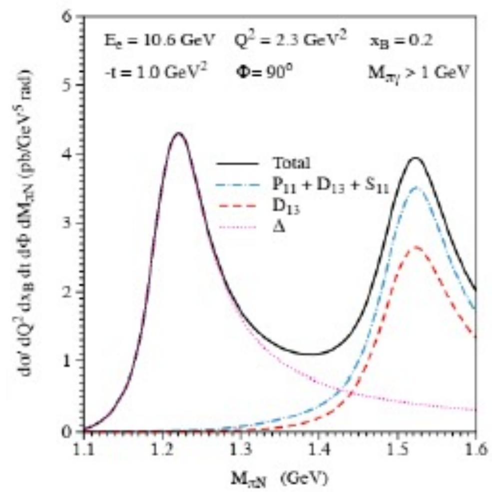

- **study in progress**
- **π^+ mainly in CD and low momentum**
- **Good agreement of BSA**
- **awaiting pass 2**

ep->enπ^+ vs. ep->eγnπ^+

ep->enπ^+

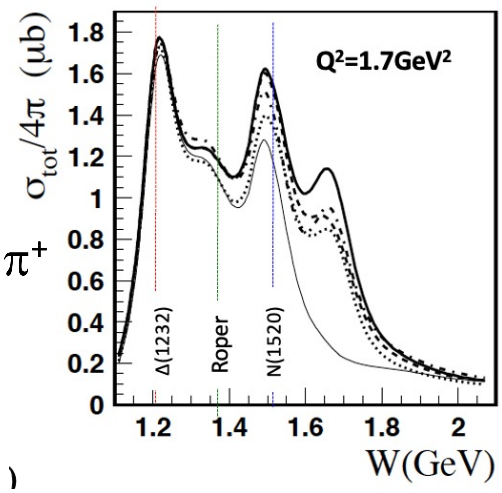

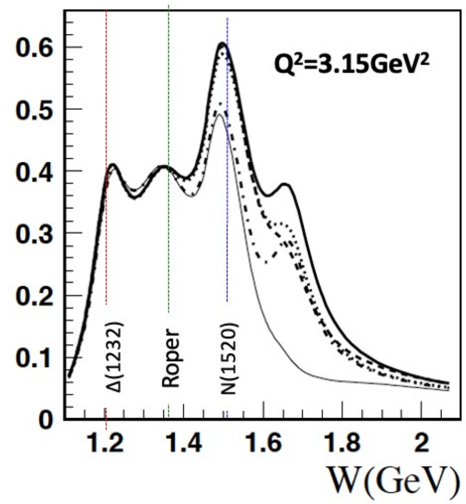

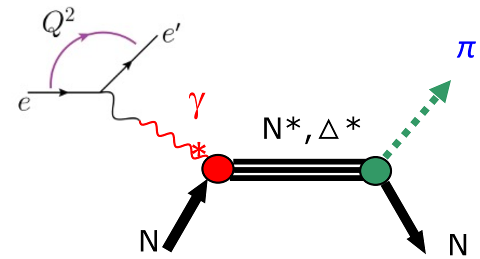

ep->eγnπ^+

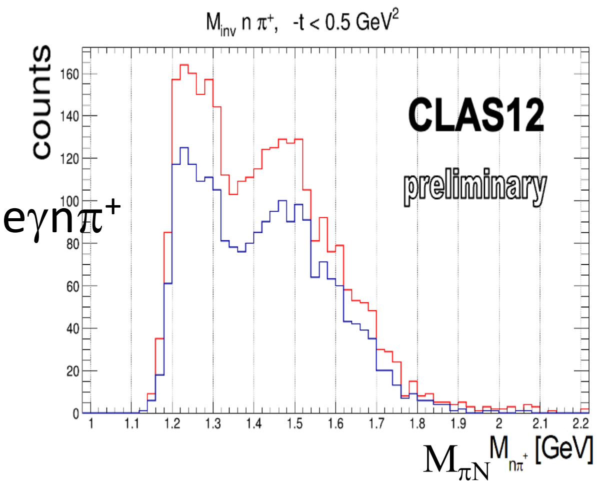

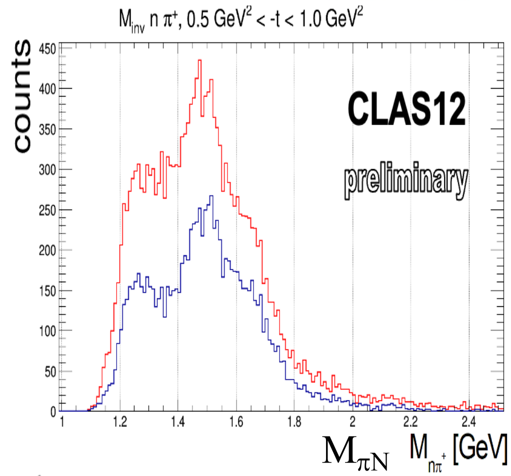

W > 2 GeV

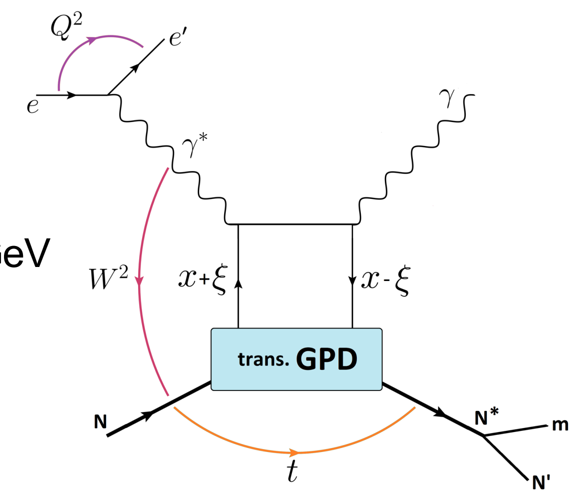

UCONN | UNIVERSITY OF CONNECTICUT

Jefferson Lab

Electron Scattering Binning Scheme

	Resonance Region	DIS Region
Inclusive Scattering	Q^2, W	Q^2, x_B
Exclusive Process (γ, π, ρ, ϕ, ..)	Q^2, W, $\cos\theta^*$, ϕ	Q^2, x_B, $-t$, ϕ

Off-diagonal DVCS or DVMP Q^2, x_B, $-t$, ϕ, $M_{\pi N}$, $\cos\theta^*$, ϕ^*

Conclusion and Outlook

1. Hard exclusive $\pi^{-}\Delta^{++}$ production has been measured with CLAS12 and provides a first observable sensitive to N->Δ transition GPDs. (Phys. Rev. Lett. 131, 021901 (2023))
2. The obtained BSA is clearly negative and ~ 2 times larger than for π^{+}
3. Transition GPDs based description of the reaction exists by P. Kroll and K. Passek-Kumericki (Phys. Rev. D 107, 054009 (2023)), but a reliable prediction of BSAs is not available due to missing experimental constraints to the transversity transition GPDs.

Outlook

1. The N->N* DVCS and N->N* DVMP processes are under investigation by scanning a wide range of invariant mass of Nπ.
2. First data on these reactions are becoming available from experiments at JLab12, but detailed strategies for their analysis and theoretical interpretation need to be developed.
3. A new proposal would be submitted to the 2024 JLAB PAC for high statistics run in 7D: Q^2, x_B, t, ϕ, $M_{N\pi}$, θ^{*}, ϕ^{*}

UCONN | UNIVERSITY OF CONNECTICUT

BACKUP

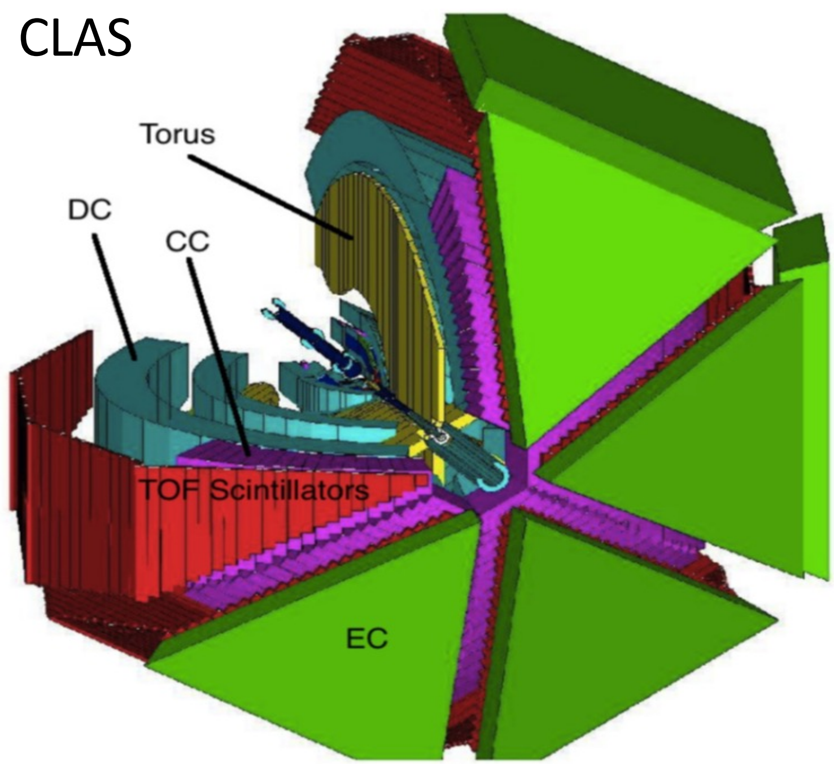

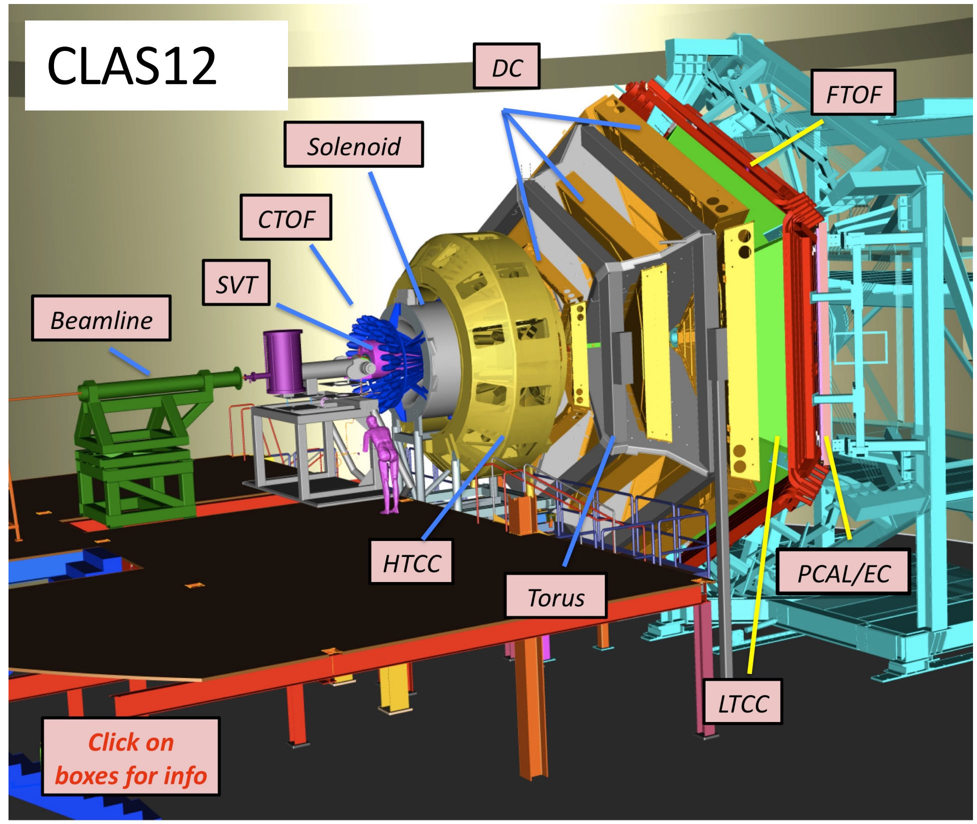

Transition Form Factors (N* Physics) at 6 GeV JLab Era → Transition GPDs (3D N* Physics) at 12-22 GeV JLab Era

Sources of Systematic Uncertainty

1. Uncertainty of the background subtraction

→ 2 sources of uncertainty: S/B ratio and sideband asymmetry

→ Both sources were varied within their uncertainty range

➔ Typically in the order of 1.5 % (low -t) - 12.5 % (high -t) (stat. ~ 12 – 25 %)

➔ Dominant sys. uncertainty for the high -t bins

2. Uncertainty of the beam polarization ~ 3.1 %

3. Effect of the extraction method and the denominator terms ~ 2.8 %

4. Acceptance and bin-migration effects ~ 2.9 %

→ Comparison of injected and reconstructed BSA in the MC

5. Radiative effects ~ 3.0 %

6. Other sources (particle ID, fiducial cuts, …) < 2.0 %

Total: 7.1 - 14.3 %

Background Asymmetry Subtraction

<u>Method 1</u>: A sideband based background subtraction

- S/B ratio from a fit of the signal shape and background asymmtry from the sideband

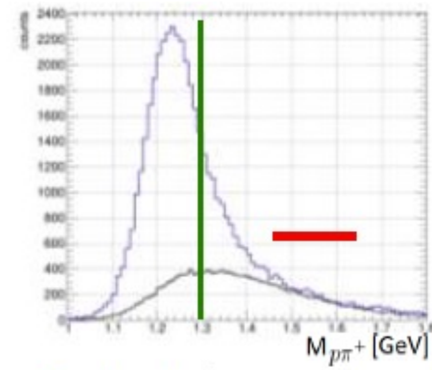

<u>Method 2</u>: A bin-by-bin background subtraction

- Fit of the $p\pi^+$ inv. mass with a „Sill“ function and a 5th order polynomial in each Q^2, x_B, -t, Φ bin.

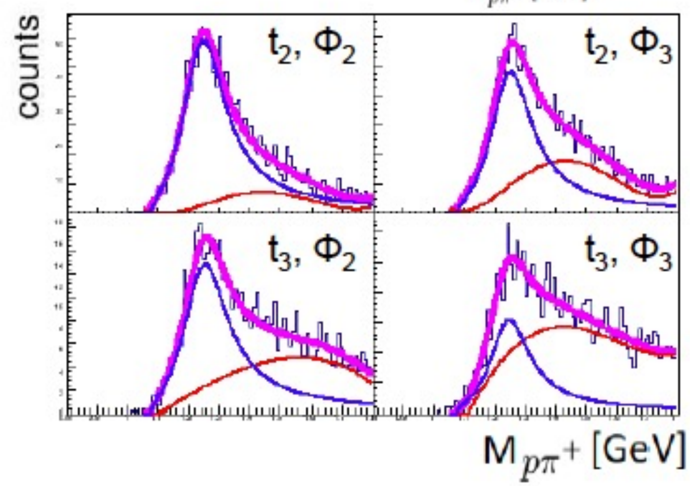

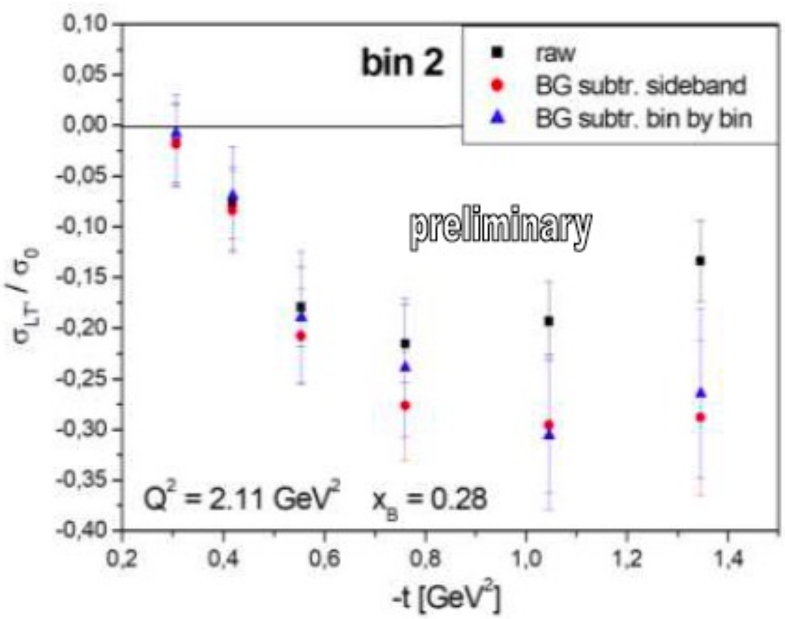

Background Subtraction

- Based on the obtained S/B ratio and based on the asymmetry of the sideband, the contribution of the non-resonant background has been subtracted.

- As a crosscheck, a bin-by-bin background subtraction has been performed with a fit of the signal and background function in each phi bin and for each helicity state.

- A good agreement of the two methods has been found.

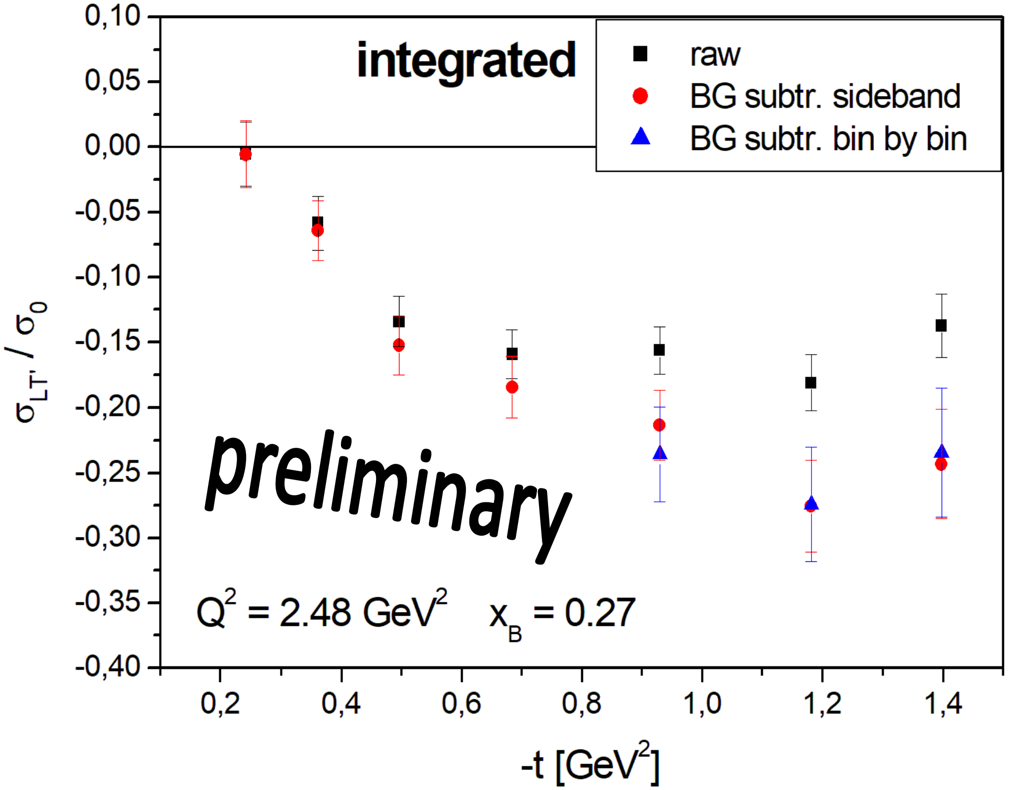

Background Subtraction

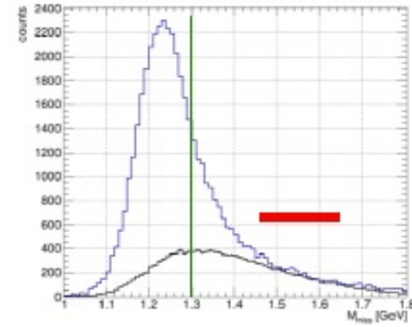

<u>Method 1</u>: A sideband based background subtraction

S/B ratio based on data - MC comparison

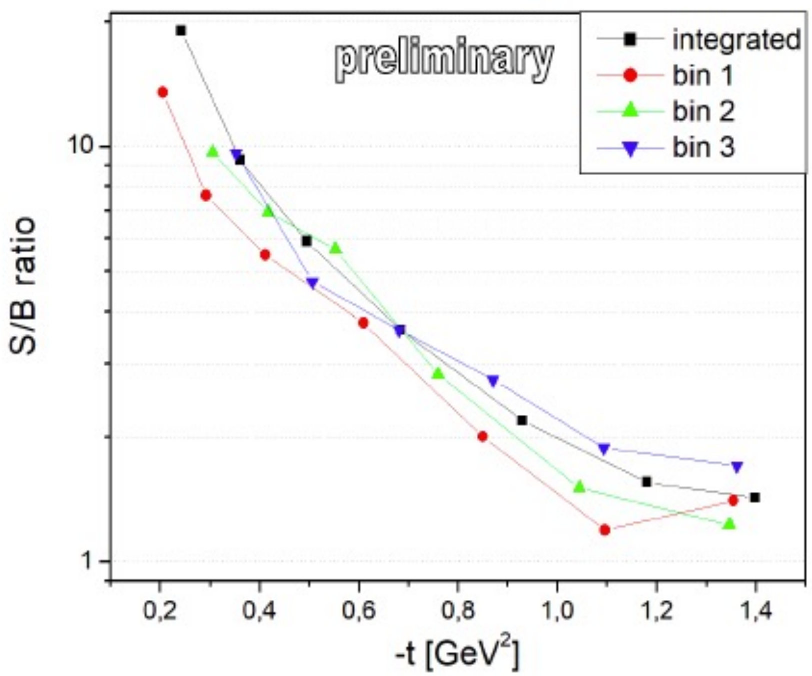

asymmetry of the sidebands

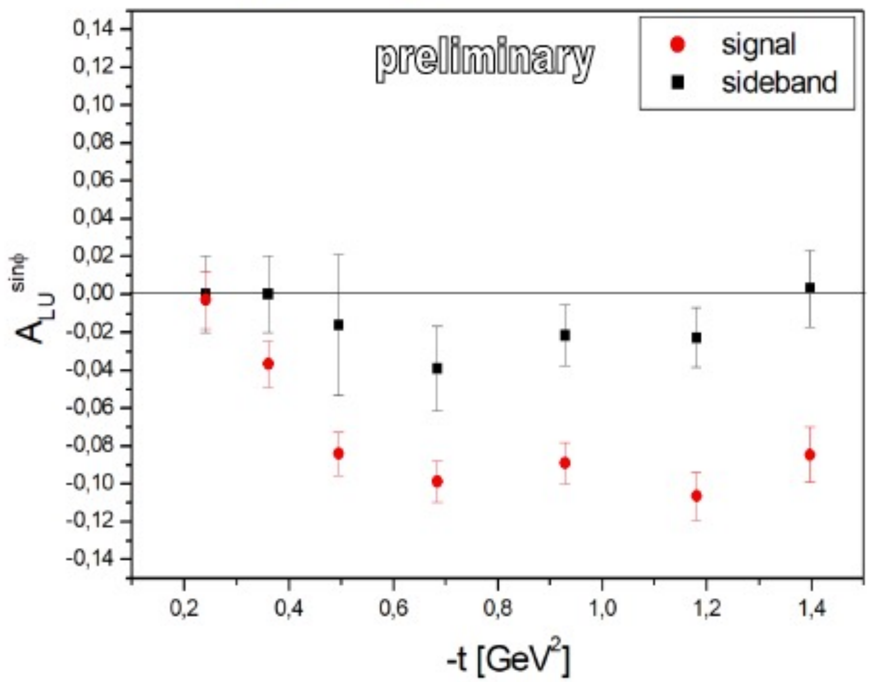

Background Subtraction

Method 2: A bin-by-bin background subtraction

• Fit of the $p\pi^+$ inv. mass with a „Sill“ function and a 5th order polynomial in each Q^2, x_B, -t, Φ bin.